anomaly for the western edge of Nubium, since the low-altitude orbital data for Ptolemaeus did not extend far enough south to cover Nubium also. If this is not the case, we are left with the conclusion that at least some of the material in the Ptolemaeus fill is of lower density than the Nubium flow, or that a deep layer of low-density regolith underlies the superficial Ptolemaeus flow. The hypothesis of a low-density flow and the similar elevations appear to agree with the hypothesis of a relatively recent high-viscosity flow in Alphonsus and Arzachel, comprising feldspathic or anorthositic material having a low density as a result of the great proportion of light, volatile elements. However, the high viscosity of such lava might not be compatible with the smooth, level floor observed in Ptolemaeus unless the temperature of the flow or of the neighboring lunar surface was great enough to permit the flow to reach a smooth level only in Ptolemaeus.

S. H. ZISK

Haystack Observatory,
Westford, Massachusetts 01886

References and Notes

1. A more complete discussion of the techniques is given in I. I. Shapiro, S. H. Zisk, A. E. E. Rogers, M. A. Slade, T. W. Thompson, *Science* **178**, 939 (1972).
2. P. M. Muller and W. L. Sjogren, *ibid.* **161**, 680 (1968).
3. W. M. Kaula, *Phys. Earth Planet. Interiors* **4**, 185 (1971).
4. Z. Kopal, "Scientific Report No. 2" (USAF contract F6105-2-68-C-0002, University of Manchester, Manchester, England, June 1970).
5. For references and an evaluation of earlier results see V. S. Kislyuk, *Sov. Astron. AJ* **14**, 487 (1970).
6. S. H. Zisk, M. H. Carr, H. Masursky, R. W. Shorthill, T. W. Thompson, *Science* **173**, 808 (1971); S. H. Zisk and T. Hagfors, "Final Report" (NASA contract NAS9-7830, M.I.T. Lincoln Laboratory, Lexington, September 1970).
7. S. H. Zisk, *Moon* **4**, 296 (1972).
8. The Haystack-Westford interferometer system was originally built for mapping the radar reflectivity of Venus. See A. E. E. Rogers and R. P. Ingalls, *Radio Sci.* **5**, 425 (1970).
9. Apollo Lunar Geology Investigation Team, *Science* **175**, 407 (1972).
10. W. K. Hartmann, *Commun. Lunar Planet. Lab. No. 24* (1964).
11. See, for example, D. E. Wilhelms and J. F. McCauley, *Geological Survey Map I-703* (U.S. Geological Survey, Washington, D.C., 1971).
12. P. Gottlieb, P. M. Muller, W. L. Sjogren, W. R. Wollenhaupt, *Science* **168**, 477 (1970); W. L. Sjogren, P. Gottlieb, P. M. Muller, W. Wollenhaupt, *ibid.* **175**, 165 (1972).
13. Lunar Orbiter IV high-resolution frame 108.
14. Thanks to G. H. Pettengill and T. R. McGetchin for useful and stimulating discussions, and to R. P. Ingalls, J. I. Levine, G. W. Catuna, and others at Haystack Observatory for assistance with the radar and data processing. Particular thanks are due A. E. E. Rogers for indispensible assistance with the interferometer and the original computer programs for processing the present moon topography data. This work was carried out at Haystack Observatory, which is operated by the Massachusetts Institute of Technology for the Northeast Radio Observatory Corporation. Support by NASA contract NAS9-7830 is gratefully acknowledged.

31 March 1972; revised 5 July 1972

Uptake and Binding of Uranyl Ions by Barley Roots

Abstract. *After undergoing the processing for electron microscopy, bound uranyl ions are revealed as characteristic electron-opaque crystals. Meristematic walls and associated vesicles become heavily labeled, while pinocytotic accumulation into vacuoles seems probable in cap cells and those just behind the meristem. The endodermal Casparian strip and suberinized lamella are effective barriers to the passage of uranyl ions.*

When seminal barley roots 20 to 30 centimeters long were placed in dilute solutions of uranyl acetate and then processed for electron microscopy (*1*), typical electron-opaque crystals were found in cell walls and, sometimes, within cells. These crystals are thought to be a uranyl complex resulting, at least in part, from the reaction of bound uranyl ions with phosphate in the buffered fixative solutions (*2*). There is no doubt that the electron-opacity is caused by the presence of uranium: omission of osmium tetroxide fixation does not affect the appearance of the crystals (*2*); the crystals are quite characteristic and easily recognizable in the electron microscope; and they are present regardless of the presence or absence of any post-staining procedure. We have used this system as part of a program to investigate the uptake and binding of electron-opaque markers at different points along barley roots (*3*).

Uranyl acetate was used in concentrations of $10^{-3}M$ or $10^{-4}M$ in aqueous solution; $10^{-3}M$ uranyl acetate is relatively toxic and exposure periods were kept below 1 hour. Electron-opaque crystals were only found in the exterior three to four layers of cortical cells, and therefore this concentration was not used further. No toxic effects were noted in roots grown for almost 1 day in $10^{-4}M$ solution, and this concentration was used for all subsequent experiments.

The apical 2 millimeters of a barley root include both root cap and meristematic zone. Our observations in the root cap generally supported those of Wheeler and Hanchey (*2*), although crystals were only seen in cytoplasmic vesicles relatively infrequently. Some walls contained much higher densities of crystals than others, peripheral walls usually being less heavily labeled. In the meristematic zone itself the presence of uranyl crystals led to extremely high opacity of many walls (Fig. 1A) although, once again, there were distinct gradations of density (Fig. 1B). Newly formed walls, even cell plates, and closely associated vesicles were the most heavily labeled of all (Fig. 1C).

The region immediately behind the meristematic zone is characterized by cells which are expanding. The endodermis is now well formed and recognizable, although the Casparian strip does not become easily recognizable until 5 to 7 mm from the tip. The cortical cells in this region 2 to 3 mm from the tip had dilated plasmalemma membranes, forming cavities between themselves and the cell wall, which were filled with crystals (Fig. 1D). Crystals were also present in vacuoles, including the vacuoles of endodermal cells (Fig. 1E). The radial walls of endodermal cells generally presented no barrier to centripetal penetration.

As soon as the Casparian strip is laid down (5 to 7 mm behind the root tip), penetration of the tracer solution beyond the outer tangential wall of the endodermal cell and the outer parts of the radial walls is completely blocked (Fig. 1, F and G). The cortical cell walls were relatively heavily labeled, as were the intercellular spaces. By 8 to 12 cm from the tip, the endodermal walls have started to undergo their typical thickening of the inner and radial sides. In some cases quite thick walled endodermal cells are found adjacent to those only possessing a Casparian strip (Fig. 1, H and J). Once again the Casparian strip is the barrier to passage of the marker inward through the cell wall, but the deposition of the "suberinized lamella," prior to further wall thickening completely precludes any further access of the marker solution to the inner edge of any part of the endodermal wall (Fig. 1, H and I).

The results described here are from experiments designed to investigate the uptake of molecules and ions by plant roots. The first few millimeters are, therefore, of comparatively little interest in this connection, although the observations made have some importance. Just behind the meristematic zone, and to a lesser degree in the root cap, micrographs have been obtained which suggest that pinocytotic activity may be taking place. On the other hand, in the meristematic zone itself the observations would generally

be interpreted to indicate that the vesicles fusing with the cell plate and new cell wall have some capacity for binding uranyl ions. It cannot be clear from a single micrograph, but some of these vesicles in close proximity with the young wall are definitely separate from it. If the free vesicles do bind uranyl ions, then these must be present in the cytoplasm for accumulation within the vesicles. In view of the fact that these vesicles probably contain pectic substances and acid polysaccharides, with which metal cations might be expected to react, this suggestion seems quite probable. It would also explain why the youngest walls were most heavily labeled in both the meristematic zone as well as within the cell cap. However the significance of pinocytotically transferring material with bound uranyl complex from the cell wall to the vacuole remains unclear, and, indeed, awaits dynamic experimentation before further progress can be made.

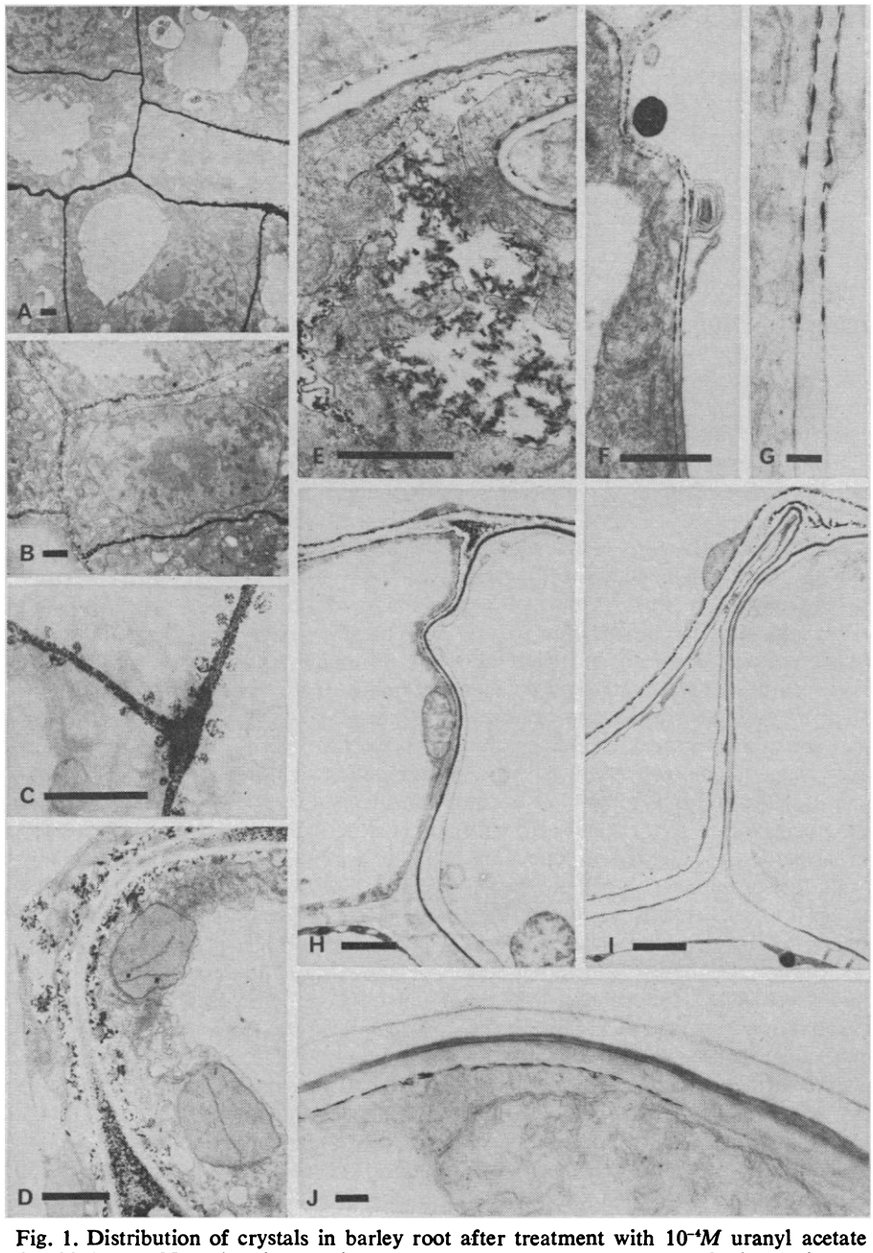

Fig. 1. Distribution of crystals in barley root after treatment with $10^{-4}M$ uranyl acetate for 22 hours. No other heavy element was present except osmium. Scale marks are equivalent to 1.0 μm except for (G) and (J) where they are equivalent to 0.1 μm. (A) Meristematic zone. Dense crystals are shown in the walls. (B) Meristematic zone. Dense deposition in newly formed wall compared to more mature walls. (C) Meristematic zone. Vesicles are assumed to be fusing with newly formed walls. Although some vesicles could be shown to be both labeled and detached, no labeled vesicles were seen distant to the wall. (D) Cell expansion zone. Crystals are present in intercellular spaces, and also in space between wall and plasmalemma. Uranyl-filled vesicles appear to be fusing with the vacuole. (E) Endodermal cell in expansion zone. The crystals in vacuole are in association with amorphous deposits normally and typically found only in the endodermal vacuole of untreated roots. (F) The 7-mm zone. Casparian strip blocks centripetal flow of tracer along the interface of the wall and plasmalemma. (G) Detail from (F). (H) Asynchronous endodermal thickening. The left-hand cell has only a Casparian strip which blocks inward movement; the suberinized lamella of the right-hand cell totally blocks access of the tracer solution to the plasmalemma. (I) Complete endodermal thickening. While the tracer can reach the endodermis it apparently cannot penetrate further. (J) Detail from (H).

It has long been suggested that the Casparian strip acts as a barrier to centripetal flow from the root cortex into the stele. However, little proof has been available. Our results show that the labeling solution cannot penetrate further than the Casparian strip or, alternatively, that there are no binding sites internal to the Casparian strip.

This second possibility is ruled out because, if the endodermis is in any way broken, then crystals are located within cell walls of the vascular cells. The Casparian strip, with its very tight binding to the overlying plasmalemma thus seems to act as a very efficient barrier to centripetal flow through the cell walls. As the endodermal cells mature further, the deposition of a suberinized lamella still further restricts inward flow of ions by preventing their access to the plasmalemma of the endodermal cell at any site whatsoever.

These results emphasize that flow through cell walls can only take place up to the Casparian strip in all except the first few millimeters of a barley root. Subsequently, ions must move from the extracellular space into the cytoplasm and pursue their inward movement via the plasmodesmata which penetrate all tangential walls. Whether the intercellular continuum is represented by the cytoplasm as a whole or, as has been suggested (*4*), by the endoplasmic reticulum/vacuole complex, remains to be seen.

A. W. Robards
Marlene E. Robb
Department of Biology,
University of York, Heslington,
York, YO1 5DD, England

References and Notes

1. Barley seeds (*Hordeum vulgare* L.) were soaked in distilled water for 6 hours and placed to germinate at 20°C in the dark on moist filter paper in a petri dish. After 2 to 3 days, the seedlings were transferred to 10 percent culture solution [R. S. Russell and J. Sanderson, *J. Exp. Bot.* **18**, 491 (1967)] and grown for 1

week in a controlled environment of 16 hour day length; 11,000 lu/m^2; air temperature 20°C; growth solution temperature 12° to 15°C. Seedlings were subsequently grown under the same conditions in full strength solution, which was changed weekly. Attached roots of 2- to 4-week-old plants were placed in an aqueous solution of uranyl acetate (10^{-3} or $10^{-4}M$) for the required period. After thoroughly rinsing in distilled water, segments were excised from different parts of the root, fixed for 6 hours in 1.5 percent glutaraldehyde buffered to *p*H 7.2 to 7.3 in 0.05*M* sodium phosphate, washed for more than 20 hours in six changes of 0.15*M* buffer, fixed for 5 hours at 4°C in 1 percent osmium tetroxide buffered to *p*H 7.2 to 7.3 in 0.1*M* sodium phosphate, and washed in 0.1*M* buffer. Dehydration was through an acetone series via propylene oxide into epoxy resin [H. H. Mollenhauer, *Stain Technol.* **39**, 111 (1964)]. Sections were cut on an LKB III ultramicrotome, picked up on uncoated copper grids and examined in AEI EM6B or Hitachi HS8 electron microscopes.

2. H. Wheeler and P. Hanchey, *Science* **171**, 68 (1971).
3. Sections were examined from the following zones: root cap (0.5 mm); meristematic zone (> 0.5 mm); expansion zone (2 to 3 mm); endodermal walls without Casparian strip (< 5 mm); Casparian strip present, but no further thickening (> 7 mm); suberinized lamella and tertiary wall deposition taking place (> 8 cm). In the latter case, there is a long zone (≃ 20 cm) within which endodermal wall thickening is very asynchronous: thin-walled cells can be found adjacent to cells with extremely well-developed walls. A full account of the development of the endodermis in barley roots is in preparation.
4. A. W. Robards, *Protoplasma* **72**, 315 (1971); D. T. Clarkson, A. W. Robards, J. Sanderson, *Planta* **96**, 292 (1971).

5. We thank the Science Research Council for supporting this work, and Dr. D. T. Clarkson for helpful discussions.

18 August 1972

Electrical Behavior of Cartilage during Loading

Abstract. *When cartilage is deformed, it becomes electrically polarized. At least two mechanisms seem to underlie this phenomenon, namely, a short-duration, high-amplitude, piezoelectric-like response and a longer-duration, lower-amplitude response secondary to streaming potentials. The polarity of articular cartilage during loading could hypothetically facilitate joint lubrication.*

Mechanically induced electrical polarization has been observed in a variety of biological systems (*1*). This polarization (charge separation) has been thought to occur mainly as a result of deformation of structural, long-chain, crystalline biopolymers, such as collagen, cellulose, protein-polysaccharides, and keratin. The precise mechanism behind this polarization is not yet clear, although "piezoelectric," pyroelectric, solid state, and electret properties have been identified in various tissues (*2, 3*). Furthermore, streaming potentials have been observed (*2*). Regardless of origin, mechanically and "hydraulically" induced electrical polarization possibly exert a major influence on the behavior of cells, ions, and charged macromolecules and on the organization of biowater (*2, 4*). In fact, growth and regeneration can be regulated electrically (*5*). This being the case, the present study was undertaken to determine the electromechanical properties of hydrated epiphyseal cartilage as an initial step in an attempt to alter its growth pattern electrically. In the process, other types of cartilage also were investigated. The investigation demonstrates that cartilage becomes electrically polarized when subjected to a deforming force and that the polarity of the polarization may have functional significance.

A total of 30 cube-shaped specimens were removed from the upper and lower femoral and tibial epiphyses of freshly killed term fetal calves, from 3-week- and 12-week-old calves, and from 10-week-old white New Zealand rabbits. The specimens included the epiphyseal plate, sandwiched between bone of the metaphysis and the ossification center (when present). Cubes of bovine epiphyses, measuring approximately 1 by 1 by 2 cm, were loaded so that the compressive force was normal to the epiphyseal plate. Compressive loads, at a rate of 10 cm/sec, were applied to the specimens with a Bytrex load cell, with an insulated tip, mounted on a pneumatically driven plunger. Electrical polarization in the specimens was detected by means of two cotton wick, Ag-AgCl electrodes, one wick contacting the epiphyseal plate, the other wick the metaphysis or ossification center. Specimens were held between electrically insulated surfaces and mounted in a Faraday cage in which the humidity and temperature were controlled. Details of the general procedure have been published previously (*6*). The amount of deformation (linear potentiometer), load, and electrical activity were recorded simultaneously with a type-R Dynograph and appropriate couplers (input impedance of the electrometer greater than 10^{10} ohms). For high-speed recordings, a Philbrick SPMD-100 operational amplifier (input impedance greater than 10^{10} ohms) was coupled to a Tektronix 564 oscilloscope.

In addition to the epiphyseal cartilages, 36 small cubes of fresh fetal and postfetal calf cartilage from the trachea, articular surfaces, menisci of the knee, and costal regions were tested. All samples were kept fully hydrated by storing in Ringer-Tyrode solution during shipment from the abattoir and during processing. Immediately prior to testing in the chamber, excess moisture was removed from the surface by blotting.

Epiphyseal samples were deformed in single steps through a range of 0.5 to 2 mm. The associated load, which initially reached values from 1 to 9 kg. decayed an average of 20 percent during the first 10 seconds and very slowly thereafter. For example, 60 seconds after the onset of a step deformation, 60 percent of the initial peak load was still present in the term calf specimens. As the specimens were deformed, electrical potentials, ranging from 0.5 to 2 mv, were recorded. The epiphyseal plate always was negative, relative to the surrounding bone of the metaphysis or ossification center. Electrical potentials decayed slowly, although at a rate faster than that generally observed for load decay. During the first 10 seconds, the initial peak potential decayed an average of 45 percent. The rate of electrical potential decay after the first 10-second period varied greatly from sample to sample, but rarely reached the baseline, even after periods in excess of 3 minutes. On release of the deforming load, a very small or no "reverse spike," indicative of a potential with a polarity opposite to that recorded on compression, was observed. This behavior differed greatly from that reported for bone (*6*). Generally, specimens with a very thick cartilaginous plate or a completely cartilaginous epiphysis (prior to the appearance of an ossification center) produced potentials of lowest amplitudes (0.5 to 1 mv). Furthermore, the decay rate of load during compression was greatest in these samples; frequently it had fallen 65 to 70 percent of the initial value at the end of the first 10 seconds.

After a complex sample, consisting of bone and cartilage, had been tested, metaphyseal and epiphyseal bone was dissected from the epiphyseal plate and each component was tested separately in compression. Electrode wicks were placed on adjacent faces of the cubes (90° from each other). Rarely were electrical polarization values of more than 100 to 200 μv recorded from the cancellous bone, while the polarization in the cartilage alone ranged from 0.5 to 1.5 mv for comparable ranges of deformation (0.5 to 2 mm). Changes in orientation of the epiphyseal plate sample, with regard to the direction of the compressive load, did not produce a significant change in voltage values.